Dalitz plot analysis of three-body fragmentation of Na_3^+ excited by He impact

D. Babikov[a)]
Theoretical Chemistry and Molecular Physics Group, Los Alamos National Laboratory, Los Alamos, New Mexico 87545

E. A. Gislason
Department of Chemistry, University of Illinois at Chicago, SES (M/C 111), Chicago, Illinois 60607-7061

M. Sizun, F. Aguillon, V. Sidis, M. Barat, J. C. Brenot, J. A. Fayeton, and Y. J. Picard
*Laboratoire des Collisions Atomiques et Moléculaires, Bât. 351, Unité Mixte de Recherche C8625, Université Paris-Sud XI, 91405 Orsay Cedex, France*

Three-body fragmentation of Na_3^+ ions to $Na^+ + Na(3s) + Na(3s)$ following excitation by He is studied experimentally and theoretically. The three reduced kinetic energies of the products in the center-of-mass are determined for each fragmentation event, and the results are displayed in a Dalitz plot. The fragmentation involves three adiabatic $^1A'$ electronic states of Na_3^+ that become degenerate at the detector. It is possible to determine the final electronic state for each event, and here we show that each of the three product states appears in a particular sector of the Dalitz plot. Theoretical and experimental Dalitz plots for the three-body fragmentation of Na_3^+ are presented, and the results are related to various mechanisms for three-body fragmentation of this system. © *2002 American Institute of Physics.* [DOI: 10.1063/1.1455623]

I. INTRODUCTION

The dissociation of an excited polyatomic molecule into three fragments is a process of great interest in molecular physics.[1–3] Recently, a few experiments have been done where all three products are detected in coincidence. One such experiment is the polar fragmentation of H_3^+ following a collision with He studied by Jaecks and co-workers,[4]

$$H_3^+ (+He) \rightarrow H^+ + H^+ + H^- (+He). \tag{1}$$
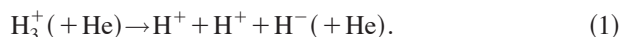
A related study of the same system was carried out by Hinojosa *et al.*[5] Continetti and co-workers[6] have used dissociative photodetachment to induce three-body fragmentation in the systems,

$$O_6^- + h\nu \rightarrow O_2 + O_2 + O_2 + e^-, \tag{2}$$

$$O_3^- (D_2O) + h\nu \rightarrow O + O_2 + D_2O + e^-. \tag{3}$$
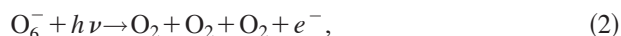
A third study involves the collisionless fragmentation of a photoexcited H_3 molecule to yield three ground state H atoms.[7] In our laboratory we have studied the collision-induced fragmentation of Na_3^+,

$$Na_3^+ (+He) \rightarrow Na^+ + Na(3s) + Na(3s)(+He), \tag{4}$$
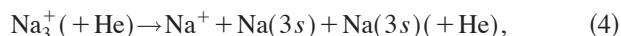
both experimentally[8,10] and theoretically.[9,10]

In the coincidence experiments described above the laboratory velocities of all three product particles are determined, and from those values the translational energies of the particles relative to their common center-of-mass can be determined. Since each fragmentation event yields three veloc-

ity vectors, a study of, for example, 10 000 dissociations will produce an enormous amount of data. The best way to display such data is by using Dalitz plots.[11] These plots have been used in the past to interpret several of the three-body fragmentation processes described above.[1–4,7]

In processes (1) and (4) it is clear that at the end there are three degenerate singlet electronic product states. [For example, in (1) the negative charge can be on any of three H nuclei; each possibility corresponds to a different electronic state.] It is also clear that early in the fragmentation process the three adiabatic electronic states are not degenerate and, presumably, the populations of the three states are not the same. As the fragmentation process evolves there is no compelling reason why the populations of the three adiabatic states should become equal as they reach the region where they are equal in energy. In a recent paper[10] we have shown for process (4) that it is straightforward both experimentally and theoretically to determine the populations of the three adiabatic states at the detector and, more importantly, that the populations are not equal.

In this paper we determine experimental and theoretical Dalitz plots for process (4). We present a more useful convention for labeling the energy axes in the plots. Finally, we show that a particular area of the Dalitz plot can be associated with each product adiabatic electronic state.

II. THEORY

A. Dalitz plots for Na_3^+ three-body fragmentation

The construction of the Dalitz plot is straightforward for three Na particles of equal mass m.[11] We begin by calculating the kinetic energy of the three fragments in the cluster

---

[a)]Author to whom correspondence should be addressed. Electronic mail: babikov@lanl.gov

c.m. frame after the collision with He. Suppose the final lab velocities of the three fragments are $\mathbf{V}_a$, $\mathbf{V}_b$, and $\mathbf{V}_c$. Then the velocity of the c.m. of the product cluster is

$$\mathbf{V}_{CM} = \tfrac{1}{3}(\mathbf{V}_a + \mathbf{V}_b + \mathbf{V}_c), \tag{5}$$

and the kinetic energy of particle i in the cluster c.m. is

$$\mathcal{E}_i = m/2|\mathbf{V}_i - \mathbf{V}_{CM}|^2. \tag{6}$$

The reduced c.m. kinetic energies of the particles are then given by

$$\varepsilon_i = \mathcal{E}_i / \mathcal{E}_{tot}, \tag{7}$$

$$\mathcal{E}_{tot} = \mathcal{E}_a + \mathcal{E}_b + \mathcal{E}_c. \tag{8}$$

Clearly the three values of ε_i sum to one. The Dalitz plot is a plot that shows as a single point the three values of ε_i for each fragmentation event. The points lie inside the tangent circle of radius 1/3 inscribed in an equilateral triangle of unit height [see Fig. 1(a)]. Each Dalitz axis i is shown as a vector of unit length drawn from the center of one side of the triangle (where $\varepsilon_i = 0$) to the opposite vertex (where $\varepsilon_i = 1$). For clarity in Fig. 1(a) each axis is shown a second time outside the triangle. Conservation of energy restricts all points to lie within the triangle; conservation of energy and momentum restricts all points to lie within the circle inscribed in the triangle.[11] Thus, the maximum possible value for ε_i is 2/3. For any point in the circle the value of ε_i is given by the perpendicular projection of the point along Dalitz axis i [see Fig. 1(a)]. We choose the reduced energy of the Na^+ product $[\varepsilon(Na^+)]$ to lie along the vertical Dalitz axis (axis Na^+), and we choose the reduced energy of the faster Na neutral $[\varepsilon(Na^{fast})]$ in the c.m. system to lie along the Dalitz axis that goes from the right side of the triangle to the vertex at the upper left (axis Na^{fast}). The energy of the slower Na neutral is denoted $\varepsilon(Na^{slow})$ and lies along axis Na^{slow}. This new convention restricts all product points to the left side of the Dalitz plot. In general, due to symmetry, any three-body fragmentation process that produces two identical products as in processes (1) and (4) requires only half the Dalitz circle to display the data. Similarly, if three identical products are produced, as in the fragmentation of H_3 to three H atoms or in process (2), only one sixth of the Dalitz circle is required.[7] Restricting the data to one-half (or one-sixth) of the circle has the advantage of doubling (or multiplying by six) the experimental signal to noise. As discussed by Braun *et al.*,[7(b)] a Dalitz plot conserves momentum phase space density. Thus, if a three-body fragmentation process produces products uniformly distributed in phase space, the corresponding Dalitz plot has a uniform density.

We note that knowledge of the three ε_i values combined with conservation of energy and momentum allows one to reconstruct the three velocity vectors relative to the c.m. velocity, $\mathbf{V}_i - \mathbf{V}_{CM}$, subject to a scaling factor that is determined by $\mathcal{E}_{tot}$. These three vectors also determine the shape of the $Na^+ - Na - Na$ triangle at the detector. (This point is discussed further in Sec. II B.) It is instructive to show the triangle shape at certain points on the Dalitz plot to indicate what type of fragmentation is taking place at those points. Several possibilities are shown in Fig. 1(b). If a point lies on an axis, then two values of ε_i are equal. For example, if a

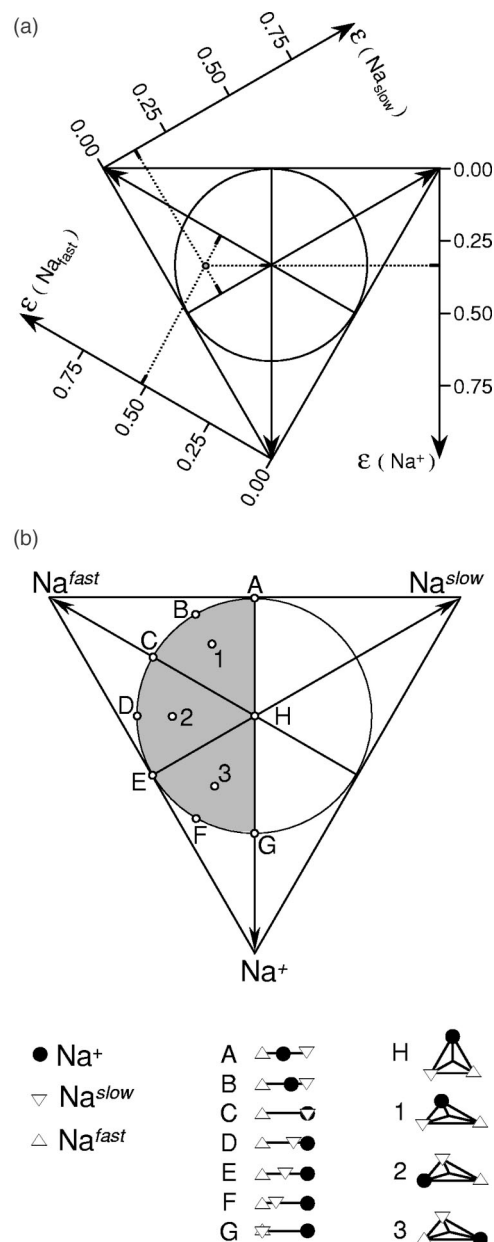FIG. 1. (a) General Dalitz plot for process (4). The tangent circle of radius 1/3 is inscribed in an equilateral triangle of unit height. Each point is determined from the values of the reduced c.m. kinetic energies ε_i ($0 \leq \varepsilon_i \leq 1$) of the three particles as defined in Eq. (7). Each Dalitz axis i is shown as a vector of unit length drawn from the center of one side of the triangle (where $\varepsilon_i = 0$) to the opposite vertex (where $\varepsilon_i = 1$). For clarity each axis is shown a second time outside the triangle. For any point in the circle the value of ε_i is given by the perpendicular projection of the point along axis i. The sum of the three ε_i equals one. The vertical axis gives $\varepsilon(Na^+)$; the axis running from lower right to upper left gives $\varepsilon(Na^{fast})$, the reduced energy of the faster Na neutral in the center-of-mass; and the axis running from lower left to upper right gives $\varepsilon(Na^{slow})$. Because of this convention for the Na energies all of the data points are found in the left half of the circle. An example point is shown, where the values are $\varepsilon(Na^+) = 0.33$, $\varepsilon(Na^{fast}) = 0.54$, and $\varepsilon(Na^{slow}) = 0.13$. (b) A number of examples of the $Na^+ - Na - Na$ triangle shape are shown below the Dalitz plot for particular points on the left hand side of the plot, which is shaded. As discussed in the text all fragmentation events that give products in the top segment of the Dalitz plot correspond to product in the ground adiabatic electronic state (state 1). Similarly, points in the middle (lowest) segment correspond to products in state 2 (state 3).

point lies on the vertical Na$^+$ axis, this means that $\varepsilon(\text{Na}^{\text{fast}}) = \varepsilon(\text{Na}^{\text{slow}})$. The three axes meet at the center of the circle, and there $\varepsilon(\text{Na}^+) = \varepsilon(\text{Na}^{\text{fast}}) = \varepsilon(\text{Na}^{\text{slow}}) = 1/3$. A point at the bottom of the circle along the Na$^+$ axis with $\varepsilon(\text{Na}^+) = 2/3$ represents the case where a fast Na$^+$ ion is produced, and the two Na neutrals separate with a very small velocity relative to each other. Similarly, a point along the Na$^{\text{fast}}$ axis with $\varepsilon(\text{Na}^{\text{fast}}) = 2/3$ at the edge of the circle corresponds to a fast Na neutral with the remaining Na and Na$^+$ separating with a very small velocity relative to each other. A third interesting limit occurs when $\varepsilon(\text{Na}^+) = 0$ at the top of the circle. In that case the Na$^+$ is produced at rest in the c.m. system, and the two Na neutrals fly apart with equal speeds but opposite directions. A comparable situation occurs when $\varepsilon(\text{Na}^{\text{slow}}) = 0$. Any point along the circumference of the circle gives three products that dissociate along a line. The Dalitz plot naturally divides into three sectors. The Na$^+$–Na–Na triangle shapes for typical points near the center of each sector are also shown in Fig. 1(b). The triangles show the relative placement of the Na$^+$ ion in the triangle. (For example, in point #1 the ion is opposite the longest side of the triangle.) In general the shape of the triangle is not intuitively obvious from the three ε_i values, and, consequently, Fig. 1(b) proves to be very useful as a reference guide for interpreting Dalitz plots for the Na$_3^+$ system.

It is common to show all experimental data in a single Dalitz plot, regardless of the $\mathcal{E}_{\text{tot}}$ value. For experiments that look at fragmentation from a known excited state,[7] $\mathcal{E}_{\text{tot}}$ has a single value. However, for experiments that use collisional activation to induce fragmentation, there will be a range of $\mathcal{E}_{\text{tot}}$ values, and it may be instructive to create Dalitz plots for different values of $\mathcal{E}_{\text{tot}}$. Alternatively, we shall see that it is useful to create various Dalitz plots based upon particular values of other experimental variables such as the deflection angle of the Na$_3^+$ in the collision with He.

B. Determination of the product adiabatic electronic state

We can determine the product adiabatic electronic state for each event of reaction (4) from the experimental coincidence data. The analysis has been described earlier;[10] only a brief summary is given here. There are three $^1A'$ electronic states involved. The three Na nuclei form a triangle. We label the nuclei a, b and c and denote the length of the triangle side opposite nucleus k as R_k. Once the particles are far apart they fly in straight lines, and the relative distances R_k are given by

$$R_k = v_k t + R_k^0. \tag{9}$$

Here R_k^0 is on the order of a few angstroms and is negligible compared to R_k at the detector. At sufficiently large t the R_k values are ordered in the same way as the atom–atom relative speeds v_k. For example, if $v_a < v_b < v_c$, then $R_a < R_b < R_c$ at large t, and this ordering is maintained until the particles reach the detector.

The diabatic state of the system (a, b, or c with energy E_a, E_b, or E_c) is identified by which nucleus (a, b, or c) has the positive charge, and this state is determined experi-

mentally. The adiabatic states (1, 2, or 3), on the other hand, are determined by the energy ordering with $E_1 < E_2 < E_3$. If the diabatic Hamiltonian matrix is set up and diagonalized, one obtains the adiabatic energies.[12] In general the positive charge is delocalized over all three Na nuclei for each adiabatic state. Once all three atom–atom distances are sufficiently large (greater than 12 Å for Na$_3^+$), however, the positive charge is fixed on one of the three nuclei, and the diabatic Hamiltonian matrix is diagonal.

As the Na$_3^+$ system evolves to larger separations R_k, the system may hop from one adiabatic surface to another at avoided crossings. We define the asymptotic region as the region where all three R_k values are sufficiently large that two conditions are simultaneously satisfied: first, the positive charge is fixed on one nucleus (i.e., the diabatic state is fixed) and, second, the R_k values are ordered in the same way as the v_k. We have shown[10] that hops between adiabatic states are forbidden in the asymptotic region, because there are no additional avoided crossings in this region and because there is no electronic coupling between the adiabatic states. It is possible to determine the one–one mapping between diabatic and adiabatic states in this region. The only important contributions to the interaction energy are the attractive ion-induced dipole potential terms between Na$^+$ and each Na, which are proportional to $1/R^4$. The total energy is the sum of these two terms. It can be proven[10] that if $R_a < R_b < R_c$, then $E_c < E_b < E_a$. This case is shown in Fig. 2. Since the asymptotic region persists to the detector, this is the mapping at the detector as well. Thus, we see that the adiabatic state can be identified by the shape of the triangle at the detector and by which vertex of the triangle corresponds to Na$^+$.

One new and very useful feature of the Dalitz plot for process (4) is that the position of a point on the plot also indicates the product adiabatic electronic state for the event. To see this consider the point labeled ''1'' in the upper sector of the Dalitz plot in Fig. 1(b) outlined by the points HABC. An examination of the triangle formed by the three Na nuclei for point ''1'' shows that the side opposite the Na$^+$ ion is the largest of the three sides. Consequently, point 1 corresponds to a product in the ground adiabatic electronic state (see Fig. 2). It is straightforward to show in fact that any point in the upper HABC sector corresponds to a product in the ground state (state 1). Similar considerations for point ''2'' in Fig. 1(b) shows that the Na$^+$ ion is opposite the second largest side of the triangle. Consequently, point ''2'' and all other points in the HCDE sector of the Dalitz plot correspond to products in the first excited adiabatic electronic state (state 2). Finally, all points in the sector HEFG including point 3 in Fig. 1(b) indicate products in the second excited adiabatic electronic state (state 3).

C. Theoretical calculations of Dalitz plots for Na$_3^+$ fragmentation

We have carried out a series of calculations for reaction (4). They have been described in detail elsewhere[9] and only a brief summary is given here. The potential energies and couplings have been calculated using the DIM procedure of Kuntz,[13] but extended as described in Refs. 9, 10, and 14. The theoretical calculation is carried out in three steps. First,

(a) $E = E_c$, ground electronic state:

(b) $E = E_b$, first excited state:
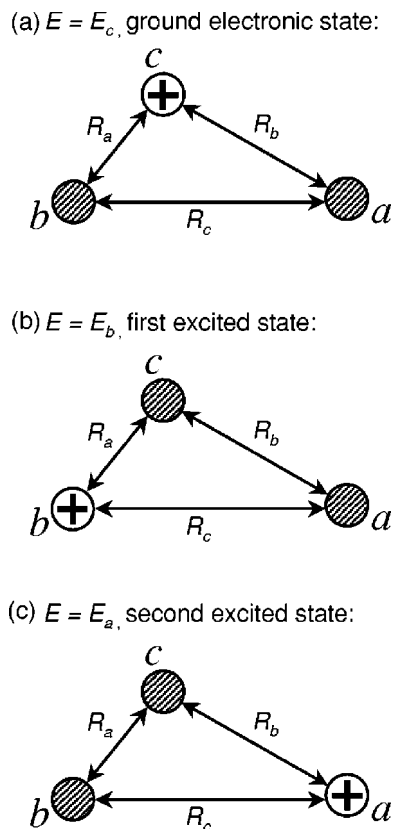
(c) $E = E_a$, second excited state:

FIG. 2. Examples of the three possible triangular configurations of the particles Na, Na, and Na^+ at the detector. The nuclei are labeled a, b, and c, and the sides opposite the nuclei are R_a, R_b, and R_c, respectively. Here $R_a < R_b < R_c$. The location of the Na^+ ion is indicated by a "+." The triangles are identical except for the location of the charge. (a) Na^+ ion at c. As discussed in the text this configuration has the lowest energy and corresponds to the ground electronic state (state 1); (b) Na^+ ion at b. This configuration has the second lowest energy and corresponds to the first excited electronic state (state 2); (c) Na^+ ion at a. This configuration has the highest energy and corresponds to the second excited state (state 3).

the Na_3^+ cluster ion classical reactant state is prepared for a fixed vibrational energy. Second, the $Na_3^+ - He$ collision is treated using the classical path approximation for the He atom and the vibrationally sudden approximation for Na_3^+. The $Na_3^+ - He$ interaction introduces couplings between the three adiabatic states of Na_3^+, and, in addition, gives an impulse to each Na nucleus. Solution of the time-dependent Schrödinger equation gives the populations of the three electronic states after the collision as well as the new momentum of each Na nucleus. Third, the fragmentation of the Na_3^+ after the collision with He is treated using the trajectory surface hopping (TSH) procedure. The trajectory may pass through one or more avoided crossings, and it may hop from one adiabatic surface to another. Earlier work[9] has shown that the vibrational energy of the Na_3^+ in the experiment is about 1 eV, so this amount was used in the present work.

The TSH calculations are carried out until all three values of R_k exceed 23 a.u. Our calculations show that at this point the positive charge is fixed on one nucleus, which defines the diabatic state of the system. The diabatic state then remains the same until the detector. Each trajectory also gives the three ε_i values for the Dalitz plot. The adiabatic electronic state at the detector is then determined from the

position of the point on the Dalitz plot [see Fig. 1(b)].

III. EXPERIMENTAL PROCEDURE

A detailed description of the experiment has been presented elsewhere.[8] Only the main features will be noted here with special attention paid to the modifications required for the multifragmentation studies. The Na_3^+ clusters are produced in an expansion at the exit of an oven heated to 820 °C. They are ionized by 60 eV electrons, accelerated to 2.4 keV and mass selected by a Wien filter. The beam is chopped at 3.3 MHz before the collision zone. The cluster ion beam crosses at 90° a "cold" He target beam produced by a supersonic expansion. The fragmented clusters then enter a parallel plate electrostatic analyzer. The ionic fragment Na^+ is deflected in the electric field and detected on the first position sensitive detector (PSD). Since only one ionic fragment per event is expected, we use a "slow" PSD (3 μs dead time for position encoding) based on a Quantar resistive anode localization device as in the previous experiments.[8] The two neutral fragments fly on a straight line through the analyzer and are detected in coincidence with the ionic fragment on a second PSD. For this experiment the earlier detector was replaced by a "faster" PSD based on a delay line localization technique. This allows detection and localization of two neutral fragments coming from the same physical event provided that the second fragment reaches the PSD at least 20 ns after the first fragment. The loss of events due to the detection dead time has been estimated for the Na_3^+ case[8(c)] to be about 5%. The present combination of a heavy projectile with a light target provides a nearly total collection of fragments on the two PSDs (4π collection in the center-of-mass reference frame). The chopper clock also triggers a multistop time-to-digital converter (TDC) that records the time of flight (TOF) of both neutral fragments as well as of the ionic fragment for each event. The velocity vectors of the three fragments are determined, in an event-by-event analysis, from their locations on the two PSDs and from their TOFs. This data allows us to construct the three values of ε_i needed for the Dalitz plot. The collision volume and the analyzing device are biased at 2.4 kV in order to get rid of the fragments produced by collision with the background gas or by evaporation of hot clusters along the incident trajectory. Because of their different energies, fragments produced

TABLE I. Experimental and theoretical distributions of product adiabatic electronic states.

State	Experimental results,[a] contributions (%)	Theoretical results, contributions (%)	
		At detector[b]	After dead-time adjustment[c]
1	42.4	39.9	44.1
2	33.1	34.0	35.8
3	24.5	26.1	20.1

[a]A total of 10 512 experimental three-body fragmentation events were observed.

[b]The calculated percentage of product adiabatic electronic states at the detector.

[c]For comparison with experiment the theoretical results have been adjusted to account for the dead time of 20 ns of the experimental detector (see text for further details).
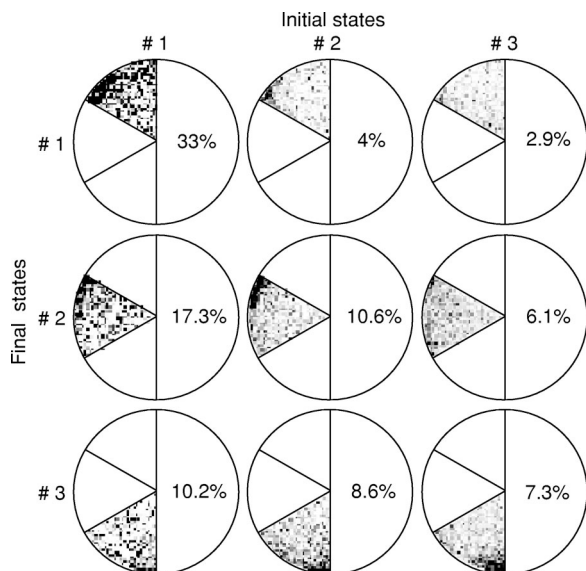
J. Chem. Phys., Vol. 116, No. 12, 22 March 2002

Fragmentation of Na$_3^+$ 4875

Initial states

1   # 2   # 3

FIG. 3. Theoretical Dalitz plots for process (4). The initial state is the adiabatic electronic state of the trajectory immediately after the Na$_3^+$ collision with He, and the final state is the adiabatic electronic state of the trajectory at the detector. The plots have not been corrected for the dead time of the experimental detector. The right-hand side of each plot gives the percentage of all three-body fragmentation events that appear in the particular Dalitz plot.
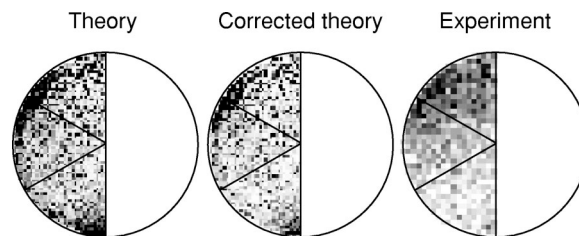
Theory   Corrected theory   Experiment

FIG. 4. A comparison of the theoretical Dalitz plot with the experimental plot for process (4). The middle circle is a theoretical plot that has been corrected for the dead time of the experimental detector.

in the collision volume are easily separated from background fragments either by the electrostatic selector or by the TOF analysis. Consequently the lab collision energy with He is 4.8 keV; the relative collision energy is 263 eV. For each set of experiments with Na$_3^+$ clusters, the electrostatic selector is tuned on the mass of the Na$^+$ fragment. Ion detection in coincidence with two neutral fragments insures an unambiguous selection of the Na$_3^+ \rightarrow$ Na$^+$ + Na + Na fragmentation pathway.

IV. RESULTS AND DISCUSSION

A summary of the product electronic state distribution is given in Table I. A total of 10 512 three-body fragmentation events were obtained in the experiments. It is seen that state 1, which corresponds to the ground adiabatic electronic state, is favored, but states 2 and 3 also have appreciable populations. Two theoretical results are given. The populations expected at the detector are shown in the third column. As discussed earlier, the neutral detector has a 20 ns dead time, so some three-body events are not detected. We have adjusted our theoretical calculations to remove all such events, and the adjusted values are shown in column four. Clearly, the detector dead time has the greatest effect on products produced in state 3. The values in column four can be directly compared with the experimental results in column two. The agreement is quite good. Further discussion of the results in this table can be found in Ref. 10.

Figure 3 gives nine state-to-state Dalitz plots obtained from the theoretical calculations. The initial state is the electronic state of the trajectory immediately after the Na$_3^+$ collides with He, and the final state is the adiabatic electronic state of the trajectory at the detector. The plots have not been corrected for the dead time of the detector. We see that the

great majority of three-body events originate in state 1. It is also apparent that there is much hopping between adiabatic states as the trajectories evolve. Finally we note that all three product states have appreciable populations, consistent with column three of Table I.

Figure 4 compares the experimental and theoretical Dalitz plots for process (4). The theoretical results on the left were obtained by adding together the nine Dalitz plots in Fig. 3. The Dalitz plot in the center is the theoretical result but corrected for the dead time of the experimental detector. This plot can be directly compared with the experimental Dalitz plot on the right. The experimental plot shows considerable intensity throughout the entire plot, but state 1 is the most populated and state 3 the least populated. One reason the entire plot is populated is that the reactant Na$_3^+$ ions have 1.0 eV internal energy. Thus, even before the collision with He the Na$_3^+$ has a wide variety of shapes different from the equilateral ground state, and also each nucleus has considerable vibrational momentum. The collision with He, in addition to possibly producing an excited electronic state of Na$_3^+$, will give each nucleus an additional impulse, further broadening the distribution of Na momenta in the three-body phase space. There is a very strong feature peaked along the Na^{fast} axis near the edge of the circle. This corresponds to a Na atom being ejected rapidly from the Na$_3^+$ followed by a slower dissociation of the remaining Na$_2^+$ species to Na and Na$^+$. Assuming that the Na$_2^+$ is randomly oriented in space as it dissociates, we would expect a peak symmetric about the Na^{fast} axis, with equal amounts of products in states 1 and 2. Such a symmetric peak is seen in both the experimental and theoretical Dalitz plots [near point C in Fig. 1(b)]. The mechanism for producing this peak has been discussed in our earlier paper.[9(d)] One of the most efficient ways for process (4) to occur is for the He to hit one of the Na nuclei in Na$_3^+$ in a hard, small impact parameter collision. Sometimes this "direct binary" collision leaves behind a stable diatomic product (Na$_2^+$ or Na$_2$), but often the diatomic dissociates giving the three-body fragmentation seen here. The "direct binary" mechanism should also produce the analogous process whereby a fast Na$^+$ ion is ejected from Na$_3^+$ followed by a slower dissociation of the remaining Na$_2$ species to Na and Na. This process should appear as a peak along the Na$^+$ axis near the edge of the circle [near point G in Fig. 1(b)]. This peak is clearly seen in the theoretical Dalitz plot. Most of the peak is lost, however, when the theoretical results are corrected for the dead time of the detector. Such a large correction is to be expected for the case that the two Na atoms have
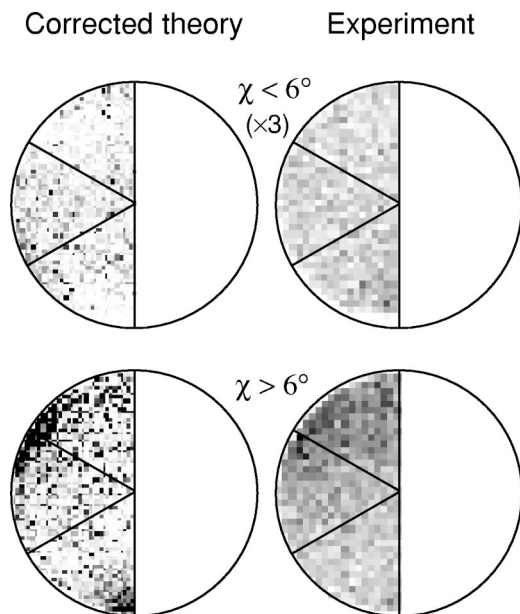
FIG. 5. Theoretical and experimental Dalitz plots for restricted values of the scattering angle χ. Here χ is the deflection angle of the Na_3^+ species in the center of mass after scattering off a He atom. (Top plots) Dalitz plots for fragmentation events with $\chi < 6°$. (Bottom plots) Dalitz plots for fragmentation events with $\chi > 6°$.

little relative separation energy. The experimental results in this region are very sensitive to the detector response[8] when two neutrals arrive at approximately the same time. In spite of this problem both the corrected theoretical and the experimental Dalitz plots show this "direct binary" peak near the bottom of the circle. This two-step fragmentation process whereby one ion or atom is ejected rapidly followed by a slower dissociation of the remaining diatomic is seen often in three-body fragmentation processes and is referred to as "sequential decay."[2]

The importance of the "direct binary" mechanism in producing the peaks seen in Fig. 4 is further supported by the theoretical and experimental Dalitz plots shown in Fig. 5. The experiments can easily determine the c.m. deflection angle χ of the Na_3^+ after scattering with the He atom. Both experiments and theory [see, for example, Fig. 7 in Ref. 9(d)] show that the χ values for three-body fragmentation separate nicely into two peaks, one sharp peak with $\chi < 6°$ and the other more diffuse peak with $\chi > 6°$. The large angle scattering occurs when the He atom hits one of the Na nuclei in a hard collision that then leads to complete fragmentation. The small angle peak, on the other hand, is seen when the He does not hit any Na nucleus hard but instead gives electronic excitation to (primarily) state 3 [Ref. 9(a)] which then yields three-body fragmentation. Figure 5 shows that the Dalitz plots for $\chi < 6°$ have a very diffuse population over the entire allowed plot, as would be expected for electronic excitation of the reactant Na_3^+. By comparison, the plots for $\chi > 6°$ show clearly the two peaks associated with "direct binary" scattering, one in the upper left part of the plot [near point C in Fig. 1(b)] and one at the bottom (near point G).

In summary, we have presented the first experimental and theoretical Dalitz plots for process (4). In fact, the calculated result is the first theoretical Dalitz plot for any three-body fragmentation process. We have demonstrated that each of the three sectors of the Dalitz plot corresponds to a different product adiabatic electronic state. This analysis can be applied to certain other three-body fragmentation experiments such as process (1). The new convention for labeling the axes of the plot has the advantage of doubling the signal to noise in the plots. All areas of the Dalitz plots have appreciable population, due in part to the fact that the Na_3^+ reactant ion is quite hot. In addition, two intensity peaks corresponding to sequential decay are observed. One corresponds to a fast ejection of Na from Na_3^+ followed by a slower dissociation of the Na_2^+ species. The other is the analogous process where a fast Na^+ is ejected followed by the slower dissociation of the Na_2. Both processes are caused by the "direct binary" mechanism whereby the fast He atom hits one Na nucleus hard and ejects it rapidly from Na_3^+, either as Na or Na^+. Two additional Dalitz plots have been presented, one for products that arise from Na_3^+ scattered at small angles and the other for Na_3^+ scattered at large angles. The first plot shows primarily fragmentation that arises from electronic excitation of the Na_3^+, whereas the second is dominated by the "direct binary" processes described above. The theoretical results agree well with the experiments.

[1] C. E. M. Strauss and P. L. Houston, J. Phys. Chem. **94**, 8571 (1990).
[2] (a) C. Maul and K. H. Gericke, Int. Rev. Phys. Chem. **16**, 1 (1997); (b) J. Phys. Chem. A **104**, 2531 (2000).
[3] R. E. Continetti, Annu. Rev. Phys. Chem. **52**, 165 (2001).
[4] L. M. Wiese, O. Yenen, B. Thaden, and D. H. Jaecks, Phys. Rev. Lett. **79**, 4982 (1997).
[5] G. Hinojosa, F. B. Yousif, C. Cingeros, J. de Urguijo, and I. Alvares, J. Phys. B **32**, 915 (1999).
[6] (a) K. A. Hanold, A. K. Luong, T. G. Clements, and R. E. Continetti, Rev. Sci. Instrum. **70**, 2268 (1999); (b) K. A. Hanold, A. K. Luong, and R. E. Continetti, J. Chem. Phys. **109**, 9215 (1998); (c) A. K. Luong, T. G. Clements, and R. E. Continetti, J. Phys. Chem. A **103**, 10237 (1999); (d) *Imaging in Chemical Dynamics*, edited by A. G. Suits and R. E. Continetti, ACS Symp. Ser. 770 (American Chemical Society, Washington, DC, 2001), p. 313.
[7] (a) U. Muller, Th. Eckert, M. Braun, and H. Helm, Phys. Rev. Lett. **83**, 2718 (1999); (b) M. Braun, M. Beckert, and U. Muller, Rev. Sci. Instrum. **71**, 4535 (2000); (c) M. Beckert and U. Muller, Eur. Phys. J. D **12**, 303 (2000).
[8] (a) J. A. Fayeton, M. Barat, J. C. Brenot, H. Dunet, Y. J. Picard, R. Schmidt, and U. Saalmann, Phys. Rev. A **57**, 1058 (1998); (b) M. Barat, J. C. Brenot, H. Dunet, J. A. Fayeton, and Y. J. Picard, J. Chem. Phys. **110**, 10758 (1999); (c) M. Barat, J. C. Brenot, H. Dunet, J. A. Fayeton, Y. J. Picard, D. Babikov, and M. Sizun, Chem. Phys. Lett. **306**, 233 (1999).
[9] (a) D. Babikov, M. Sizun, F. Aguillon, and V. Sidis, Chem. Phys. Lett. **306**, 226 (1999); (b) D. Babikov, E. A. Gislason, M. Sizun, F. Aguillon, and V. Sidis, *ibid.* **316**, 129 (2000); (c) D. Babikov, E. Gislason, M. Sizun, F. Aguillon, and V. Sidis, J. Chem. Phys. **112**, 7032 (2000); (d) D. Babikov, E. A. Gislason, M. Sizun, F. Aguillon, and V. Sidis, *ibid.* **112**, 9417 (2000); (e) D. Babikov, Y. J. Picard, F. Aguillon, M. Barat, J. C. Brenot, H. Dunet, J. A. Fayeton, V. Sidis, and M. Sizun, in *Imaging in Chemical Dynamics*, edited by A. G. Suits and R. E. Continetti, ACS Symp. Ser. 770 (American Chemical Society, Washington, DC, 2001), p. 326.
[10] E. A. Gislason, D. Babikov, M. Sizun, F. Aguillon, V. Sidis, M. Barat, J. C. Brenot, J. A. Fayeton, and Y. J. Picard, Chem. Phys. Lett. **341**, 568 (2001).
[11] R. H. Dalitz, Philos. Mag. **44**, 1068 (1953).
[12] V. Sidis, in *Advances in Chemical Physics Series, State-Selected and State-to-State Ion–Molecule Reaction Dynamics, Part 2: Theory*, edited by Michael Baer and C. Y. Ng (Wiley, New York, 1992), p. 73.
[13] P. J. Kuntz, Mol. Phys. **88**, 693 (1996).
[14] S. Magnier, thesis, Universite Paris-Sud, Orsay, France, 1993.